COBRA: From industrial to medical surgery with slender continuum robots

David Alatorre Troncoso, Jose A. Robles-Linares, Matteo Russo, Mohamed A. Elbanna, Samuel Wild, Xin Dong, Abdelkhalick Mohammad, James Kell, Andy D. Norton, Dragos Axinte

***Abstract*—The maintenance of critical industrial components is often hindered by limited access, tortuous passages, and complex geometries. In highly constrained environments, inspection tasks are currently performed with borescopes, but even skilled operators struggle with hard-to-reach targets and the limited mobility prevents in-situ repair when defects are identified. Thanks to an active shape control, snake-like and continuum robots can outperform borescopes for short range inspection as well as enable intervention. However, their actuation technology limits their scalability in length, as longer bodies pose control challenges due to their intrinsically low stiffness and space constraints. To overcome the limitations of both borescopes and continuum robots, we here propose a modular design at their intersection, with both active tendon-driven and passively flexible segments. The main elements of the novel design, including actuation and control interface, are described, and the system is demonstrated in scenarios for aerospace assets, nuclear installations, and robot-assisted surgery.**

***Index Terms*—Continuum robots; design; mechanisms and actuation; industrial robotics; robotic surgery.**

I. Introduction

Inspection, maintenance and repair are critical to achieve safety and reliability in capital-intensive infrastructures, such as aircraft, power plants, and telecommunication networks. However, these operations often involve narrow, complex environments with no direct access. For example, the components within a gas turbine can only be accessed through narrow channels such as borescope ports and a reach of several meters [1][2]. Similarly, the key components of a power generator (e.g. stator core) can only be inspected through narrow passages over a significant reach [3]. By providing remote visual feedback and with a cross section that can be as small as 4 mm, borescopes are currently the state-of-the-art solution for in-situ inspection in these environments. This technology, however, has significant limitations: first, the single degree of freedom (DoF) that controls tip bending is not sufficient to intervene on a defect; further, the difficulty in positioning the borescope camera with respect to the inspection target leads to a low defect detection rate [4]; finally, only a skilled operator can manually drive the borescope through a cluttered environment and, even then, the procedure is slow and hindered by the lack of control over the tool's shape. Thus, if damage is detected, components might need to be disassembled and repaired separately, leading to long downtimes.

For these reasons, maintenance robots have been proposed to perform these inspections, aiming at a significant increase in safety and efficiency by enabling teleoperation, automated detection, and in-situ repair. Since conventional industrial robots cannot navigate the intricate geometries of aeroengines, power plants, and similar environments, snake-like continuum robots have been developed for these applications. By routing tendons through slender, flexible bodies, continuum robots can achieve full control over their shape by pulling and releasing these tendons, which act like antagonistic muscles, from the base of the robot, deployed outside the inspection environment [5][6][7]. In the last decade, tendon-driven continuum robots have been demonstrated on real-case scenarios, such as laser operations [8] and coating repair [9] in aeroengines, exploration and inspection of unknown cluttered environments for nuclear decommissioning [10][11], and also robotic surgery [12][13].

When compared to borescopes, the main advantage of continuum robots manifests by shape control, which enables intervention and significantly improves navigation. However, the length of a continuum robot is not as scalable as in borescopes, due to the intrinsic limitation of tendon-driven designs: each independent segment of a continuum robot requires three or more cables for two DoF [14]. Therefore, longer robots require many cables routed through their bodies, increasing their cross-section. Similarly, fluid-driven, concentric needle, and other continuum robot architectures encounter equivalent barriers to scalability due to the additional space required to drive each active segment. This link between mobility and size constrains length, and this constraint is further worsened by low stiffness, resulting in high deflections under small payloads [15]. Furthermore, both endoscopes and continuum robots currently require skilled operators.

We here present a near-industrialized COntinuum roBot for Remote Applications (COBRA) at the intersection of borescope and continuum robot technologies, overcoming key inherent weaknesses of both. As reported in Section II, this new design employs both tendon-driven and passive segments to achieve high dexterity at a long reach (over 5m) while maintaining a cross-section diameter of less than 9mm. Control over the passive segments is achieved with an external mechanism that controls the axial translation and rotation of the robot at the entrance of the target environment, emulating the manual action of a borescope operator. The active segment is controlled by an

Submitted 15/07/2022.
This work was supported by Innovate UK Grants 104066 (COBRA) and 51689 (REINSTATE), University of Nottingham EPSRC IAA Grant RA45DV (Medical-COBRA) and Rolls-Royce plc.

D. Alatorre, J.A. Robles-Linares, M. Russo, M.A. Elbanna, S. Wild, X. Dong, A. Mohammad, and D. Axinte are with the Faculty of Engineering, Univ. of Nottingham, Nottingham NG8 1BB, UK (dragos.axinte@nottingham.ac.uk).
J. Kell and A. Norton are with Rolls-Royce plc, PO Box 31, Derby DE24 8BJ, UK.

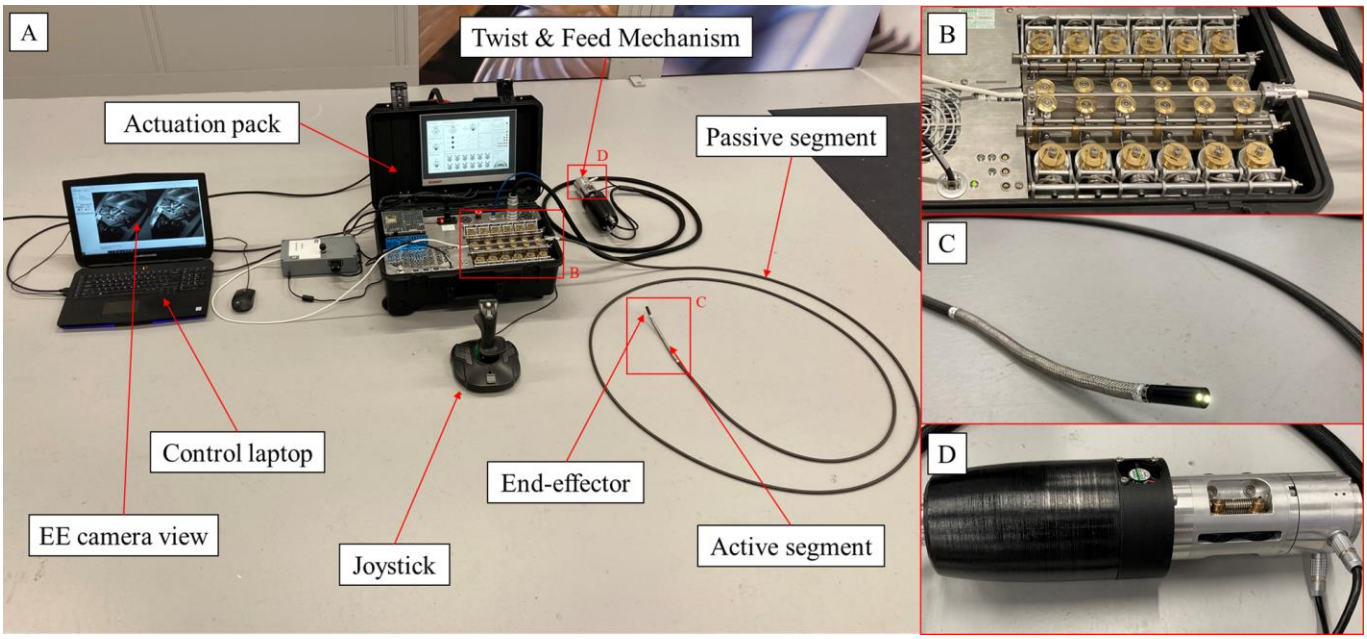

Figure 1. COBRA system overview: a. Setup with control laptop, joystick controller, 5m continuum robot with active (light grey) and passive (dark grey) segments, actuation pack for the tendon-driven active segment, and twist & feed mechanism for the passive segment; b. Pulleys for tendon driving and routing in the actuation pack; c. The 6-DoF active segment with a camera end-effector (EE); d. Linear and rotary stages of the twist & feed mechanism.

actuation unit that pulls and releases the tendons through rotary motors. A user-friendly interface, described in Section III, enables easy motion control through a joystick. As outlined in Section IV, COBRA has been tested in industrial scenarios, including an aeroengine compressor and pipes representing a nuclear power installation. The flexibility of the novel system is also highlighted by a medical application, with a specific end-effector (EE) designed for throat surgery. These demonstrations highlight how COBRA improves borescope and continuum technologies by merging the advantages of both.

II. Design

As shown in Figure 1, COBRA is divided into five subsystems:

- A Continuum Robot with three tendon-driven active sections with two bending DoF each, and passive segments, which are compliant and bend passively under external loads. The hollow body contains an inner channel for the connections required by the EE (e.g. signal, power, fluid pressure).
- A compact and truly portable Actuation Pack that drives the active segments of the continuum robots by actuating tendons through pulleys connected to rotary motors.
- A miniaturized Twist & Feed Mechanism, mimicking the behavior of a borescope operator, which drives the passive body of the robot through a rotary and linear stage, twisting the robot around its backbone axis and pulling it into or out of the inspection environment.
- Control hardware, including a PLC for low-level control and a laptop for high-level control and visual feedback.
- A joystick interface, which drives the robot with a user-friendly mapping that can be taught in a few minutes, opening these technologies to unskilled operators.

In this section, the design of COBRA is discussed, with a focus on the mechanical solutions for the continuum robot, the actuation pack, and the twist & feed mechanism.

A. Continuum robot

The active shape control of continuum robots has clear advantages when operating in fully suspended configurations (e.g. from ceiling to ground) and allows for navigation through complex paths. However, actuation technologies often limit the length and number of independently drivable segments. Conversely, passive borescopes are manually guided by pushing them into cluttered environments, combining axial translation and rotation to overcome obstacles. Despite the lack of control over a borescope's shape, navigation is made possible by narrow passages that "force" the system along the desired path. However, complex geometries and sharp turns can easily prevent a borescope from moving forward.

The continuum robot of the COBRA system aims at taking the best of both: with its long passive segments, it can benefit from the environmentally guided navigation strategy of borescopes without the stricter length constraints of conventional continuum robots; at the same time, the plurality of active tendon-driven segments provides the additional mobility that borescopes lack. The design of both passive and active segments is illustrated in Figure 2.

The passive segment could be as long as required, although friction losses limit its length in practice. Its main structural component is a thin rubber-coated braided monocoil tube at the outer surface (Fig. 2a), braided to minimize deformation under torque. Internally, coil springs serve as Bowden outer cables for the tendons and help to minimize friction when actuating the active segments. The remaining space can be used to deliver power, signals, fluid pressure, etc. to the EE.

The active segment is a tendon-driven, multi-backbone continuum robot with pivot disc vertebrae that roll onto each other (Fig. 2e). At the terminal vertebra of each independent section of the active segment (Fig. 2f), four stainless steel wire rope tendons are fixed in antagonistic pairs to control two bending DoF. Each tendon terminates with a metal sphere created by melting the tendon material with a welder. A braided sleeve encloses the active segment to provide torsional stiffness and protect the robot.

While in the reported example the prototype has a single passive segment followed by a single active segment with three sections, different combinations of these elements can be used to meet a large variety of requirements. For example, an intermediate active segment with one or two sections splitting the passive segment can provide improved reach and mobility partway through the passive segment.

B. Actuation pack

The actuation pack, shown in Figure 3, drives the active segment(s) of COBRA by pulling and releasing the tendons. Each actuation tendon is routed from the robot's passive segment (Fig. 3a) into an idle pulley without crossing any other tendon thanks to a staggered pulley layout (Fig. 3b). From there, the tendon's extremity is fixed through shape locking into an actuated pulley that is directly driven by a rotary motor (Fig. 3c). The tendons are coupled in antagonistic pairs (Fig. 3d), each one of which is driven with opposing actuation. The chassis of each motor is mounted on a pivoting structure and connected to a load cell onto which the tension of each tendon is directly transmitted: in this way, force feedback can be achieved to avoid tendon failure.

C. Twist & feed mechanism

The twist & feed mechanism, in Figure 3, has been designed to imitate the behavior of a borescope operator. As such, its motion requirements have been extracted from data from a borescope inspection performed by a skilled operator on an aeroengine. An optical motion sensor (400 DPI, 63 µm pixel size) has been installed on the borescope port of the aeroengine to record insertion and twist motion, corresponding to the sensor's Y-

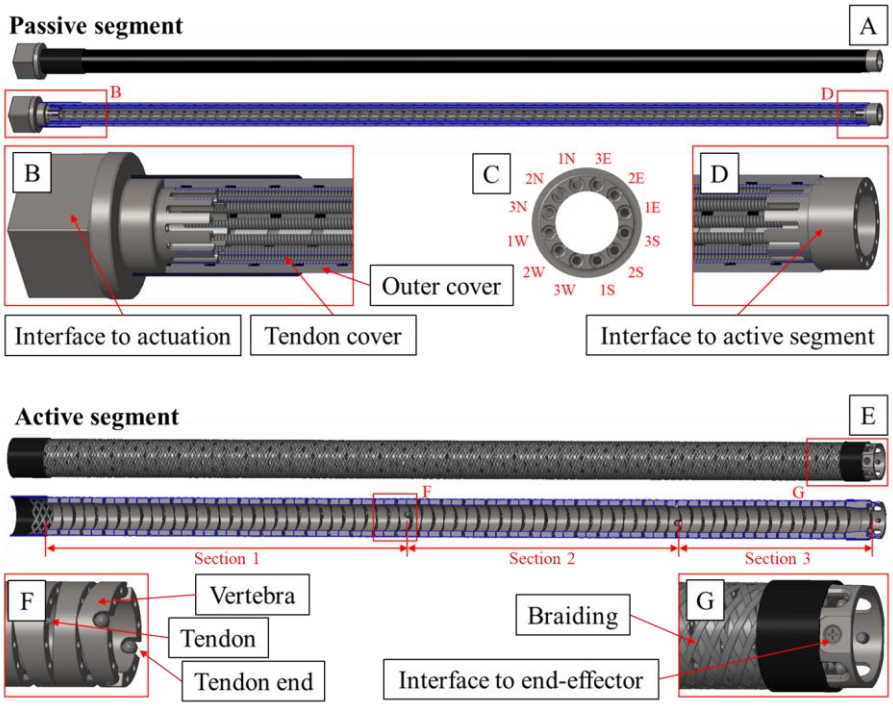

Figure 2. Continuum robot design: a. Passive segment design, with spring guides that act as tendon cover and a flexible outer cover; b. Mechanical interface between actuation pack and passive segment; c. Tendon layout in a cross-section of the robot; d. Mechanical interface between passive and active segment; e. Active segment design, with vertebrae with rolling surfaces, holes for driving tendons, and a central channel for EE delivery, and external braiding; f. A terminal vertebra of a section, with sockets for fixing tendon ends; g. Mechanical interface for the connection to the EE.

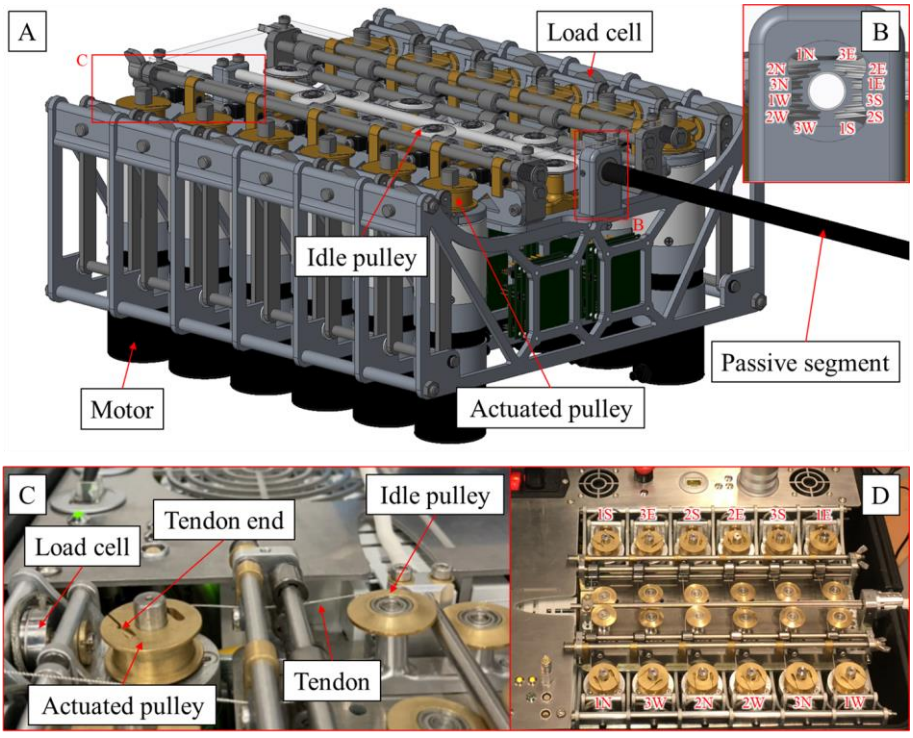

Figure 3. Actuation pack design: a. System overview, with pulleys for routing (passive) and driving (actuated) tendons, a rotary motor for each tendon, and load cells to measure tendon tension; b. Detail of tendon routing layout at the interface to the passive segment of the continuum robot; c. Close-up of the actuation unit for a single cable; d. Tendon routing layout through pulleys up to motors.

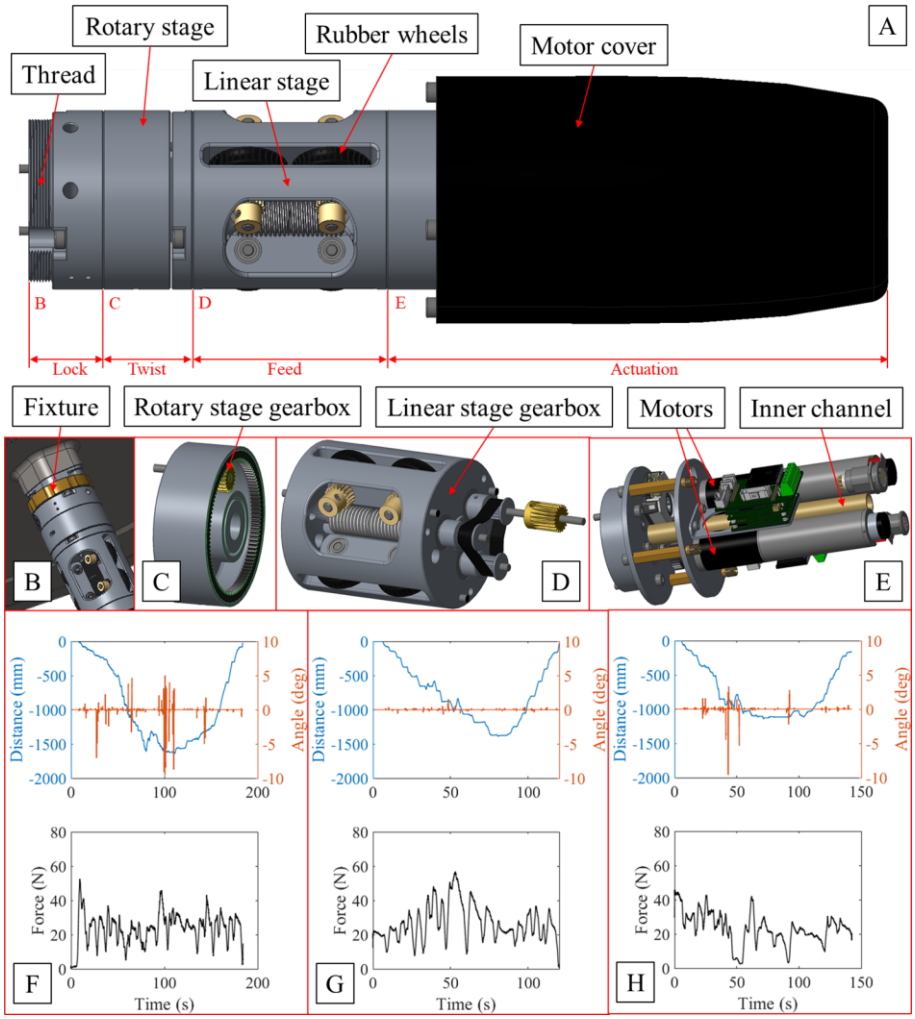

Figure 4. Twist & feed mechanism design: a. System overview, with a thread for robot deployment, a rotary stage to twist the passive segment around its backbone axis, and a linear stage to translate ("feed") the robot along its backbone axis; b. Example of twist & feed mechanism deployment; c. Rotary stage gearbox; d. Linear stage gearbox, with rubber wheels to push the robot into, or out of, the inspection environment; e. Actuation unit with motor and drivers; f-h. Acquired motion and force range for three borescope operations in aeroengines.

and X-axes acquisitions, respectively. At the same time, the driving force and torque have been measured with a pressure-sensitive pad on the endoscope grip.

The results of these acquisitions (three examples reported in Fig. 4f-g) show that a rotational range of 20deg is sufficient to achieve a complete navigation process, whereas a safe grip on the borescope is ensured with a force of 60N. The insertion distance in the plots has been acquired for completeness, but it significantly varies with operation and tool length. As such, this example twist & feed mechanism was designed according to three main requirements: rotational motion of more than 20deg; endless translation distance, provided by rubber wheels that grab the outer surface of the continuum robot; and grasping force over 60N, obtained through a calibrated interference fit between the rubber wheels and the robot.

The resulting design, illustrated in Figure 4a, is made of four main parts: a locking section, which is fixed through a threaded connector onto the target environment and contains optical motion and presence sensors (Fig. 4b); a rotary stage that provides the twisting motion (Fig. 4c); a linear stage with rubber wheels that drag the continuum robot (Fig. 4d); and a case with the motors (Fig. 4e). Given the location of the motors on the back of the twist & feed mechanism, driving motion is transmitted through a gearbox at the rotary stage (Fig. 4c), and a belt and worm gear system for the linear stage (Fig. 4d). A hollow metal tube ensures smooth low-friction motion for the robot's body throughout the twist & feed mechanism (Fig. 4e).

Other continuum robots, in addition to active control over their whole shape, employ rotary and linear stages to achieve follow-the-leader motion [10][12]. This is however achieved by moving the entire actuation pack for the tendon driven section with these base stages [8][9], requiring overengineered or bulky motors. Conversely, COBRA's design is unique in "dragging" the robot throughout its linear and rotary stage while still allowing a static actuation pack, thus significantly reducing overall system size. This feature also enables the separate deployment of the two actuation units when both kinds of controlled motion (active and passive segments) are not needed together for a given operation (e.g. acting as a teleoperated borescope with twist & feed mechanism only, or deploying the robot manually while actuating the active segment at the tip).

III. Control

In this section, the control system for COBRA is explained with its four main elements: first, the active segment is modelled with a piecewise constant curvature model; then, tendon actuation is discussed with a focus on tension feedback and backlash and stretch compensation; a novel efficient algorithm for tip-following motion is presented; finally, a human-machine interface is developed with a user-friendly mapping of the robot's motion variable onto a joystick controller.

A. Continuum robot modelling

The active segments of COBRA have been modelled with a piecewise constant curvature model, which describes a continuum robot as *n* serially connected sections that can be independently bent in any direction with constant curvature in space [7]. This kinematic model is simple and efficient, enabling real-time control for a smooth response to joystick commands. Key assumptions include a continuous differential along the backbone curve, with consecutive sections sharing the same backbone tangent at their common point, and a rigid

cross-section at any backbone length, always normal to the backbone tangent. A fixed frame $\{S_0\}$ is defined at the base of the active segment, with n further frames $\{S_i\}$ at the end of each of the n sections (Fig. 5a). A homogeneous transformation $\boldsymbol{T}_{\boldsymbol{i-1}}^{\boldsymbol{i}} \in SE(3)$ from $\{S_{i-1}\}$ to $\{S_i\}$ can be written as

$$\boldsymbol{T}_{\boldsymbol{i-1}}^{\boldsymbol{i}} = \begin{bmatrix} \boldsymbol{R}_{\boldsymbol{i-1}}^{\boldsymbol{i}} & \boldsymbol{t}_{\boldsymbol{i-1}}^{\boldsymbol{i}} \\ \boldsymbol{0}_{\boldsymbol{1\times 3}} & \boldsymbol{1}_{\boldsymbol{1\times 1}} \end{bmatrix}, \quad (1)$$

where $\boldsymbol{R}_{\boldsymbol{i-1}}^{\boldsymbol{i}} \in SO(3)$ is the rotation and $\boldsymbol{t}_{\boldsymbol{i-1}}^{\boldsymbol{i}} \in \mathbb{R}^3$ is the translation along the section circle arc. This transformation is conventionally parametrized by direction of bending φ and bending angle ϑ. Thus, the rotation from $\{S_{i-1}\}$ to $\{S_i\}$ is

$$\boldsymbol{R}_{\boldsymbol{i-1}}^{\boldsymbol{i}} = \mathrm{rot}_z(\varphi_i) \cdot \mathrm{rot}_y(\vartheta_i) \cdot \mathrm{rot}_z(-\varphi_i), \quad (2)$$

and the corresponding translation is expressed as

$$\boldsymbol{t}_{\boldsymbol{i-1}}^{\boldsymbol{i}} = \frac{\ell_i}{\vartheta_i} \begin{bmatrix} \cos\varphi_i(1-\cos\vartheta_i) \\ \sin\varphi_i(1-\cos\vartheta_i) \\ \sin\vartheta_i \end{bmatrix}, \quad (3)$$

where ℓ_i is the length of the backbone from $\{S_{i-1}\}$ to $\{S_i\}$. Once defined the shape of the backbone through these equations, the length of each tendon is required to actuate the robot. The length of each of the 12 tendons in the reported example is defined as l_{ij}, where $i = \{1, 2, 3\}$ represents the section at which the tendon ends and $j = \{\mathrm{S}, \mathrm{E}, \mathrm{N}, \mathrm{W}\}$ represents the routing position of the tendon in the section (south, east, north, west), working in antagonistic S-N and E-W pairs. The pose of each tendon in a vertebra is defined by the angle α_{ij} (Fig. 5b) around the z-axis of the local frame. As a single tendon is routed in each hole of a vertebra, the corresponding pairs for consecutive sections are shifted by a 30deg angle (Fig. 2c).

Assuming that each tendon is routed at a constant distance from the central backbone of the robot, defined by radius r_0, its change in length along the i^{th} section $\Delta l_{ij,i}(t)$ when moving from a straight backbone position $(\vartheta_i(0) = 0)$ to a bent configuration defined by $\big(\vartheta_i(t), \varphi_i(t)\big)$ can be computed as

$$\Delta l_{ij,i}(t) = l_{ij,i}(t) - \ell_i = r_0 \vartheta_i(t) \cos\Big(\alpha_{ij} - \varphi_i(t)\Big) \quad (4)$$

By repeating (4) for all tendons and sections, an input-output relationship between tendon input $\Delta l_{ij} = \sum_{i=1}^{n} \Delta l_{ij,i}$ and motion parameters $\big(\vartheta_i(t), \varphi_i(t)\big)$ can be obtained.

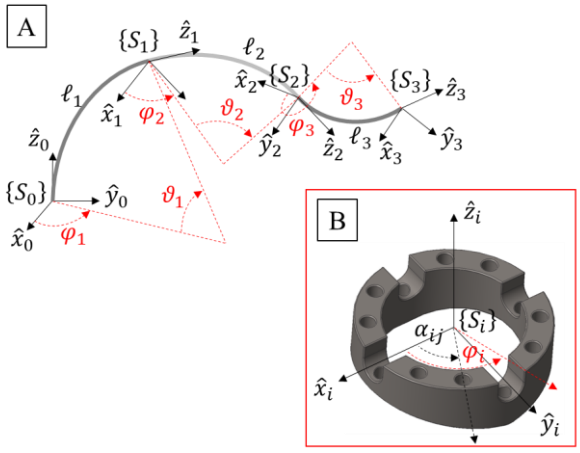

Figure 5. Active segment modelling: a. A piecewise constant curvature model for a 6-DoF, 3-section active segment; b. Model of a vertebra with geometrical parameters for tendon routing.

Two additional active DoFs of the robot are controlled by the twist & feed mechanism: twist angle $\varphi_0(t)$, which rotates the base frame of around the backbone axis, and the exposed length of the robot $\ell(t)$, defined as the backbone length inserted in the environment. As such, the example prototype can actively control 8 DoFs. However, different combinations of active and passive sections can result in a higher or lower mobility.

B. Tendon control

The model presented above estimates the change in length in each tendon required to achieve a desired motion. However, this model does not consider statics, and tendons must be always tensioned to ensure motion controllability (force closure, [16]). A closed-loop control with tension feedback is thus needed to satisfy this condition as well as avoid tendon failure due to excessive load. This feedback is obtained by the load cells installed in the actuation pack (Fig. 3) and enables not only tension tracking but also stretch and backlash compensation.

The stretch compensation can be applied from the pulley by multiplying actuation motion by a factor that can be either statically defined or dynamically estimated from the constitutive relationship of the material (i.e. computing the strain of each tendon from load cell measurement). Therefore, the rotation of each tendon motor $q_{ij}(t)$ is computed as

$$q_{ij}(t) = k_s \frac{\Delta l_{ij}(t)}{r_p}, \quad (5)$$

where r_p is the radius of the actuated pulley (Fig. 3c), k_s is the stretch factor (defined empirically by the operator and adjustable during operation), and t is time. As friction increases exponentially with total curvature, variable friction related to the accumulated curvature of the passive section and Bowden cables makes static or dynamic stretch compensation more challenging and poses a practical limit to how convoluted a path can be traversed without compromising control authority.

The backlash compensation maintains tension in antagonistic tendon pairs to prevent tendons from falling off pulleys and Bowden cables from becoming dislodged from their fittings. Each time a pair of motors changes its direction of motion, an additional motion of Δl_s is added to both actuators to ensure force closure is maintained. The value of Δl_s depends on the total robot length and is currently calibrated experimentally rather than modelled.

C. Follow-the-leader algorithm

A lightweight discrete algorithm has been developed to enable follow-the-lead deployment [17], as shown in Fig. 6. The robot's whole backbone length ℓ_0 can be discretized into short discrete intervals $\Delta\ell$ (e.g. 1mm for the reported example). While feeding the robot in the workspace, the exposed length of the robot $\ell(t)$ (acquired by the optical sensor on the feed axis) increases, and the current actuation of the active segment is recorded for each $\Delta\ell$ of exposed length and stored in a discrete array. By assuming that the passive segment follows the active one because of environmental constraints, the shape of the whole robot can be indirectly acquired by recording actuation variables during deployment. When extracting the robot, the stored values replicate the active motion backwards.

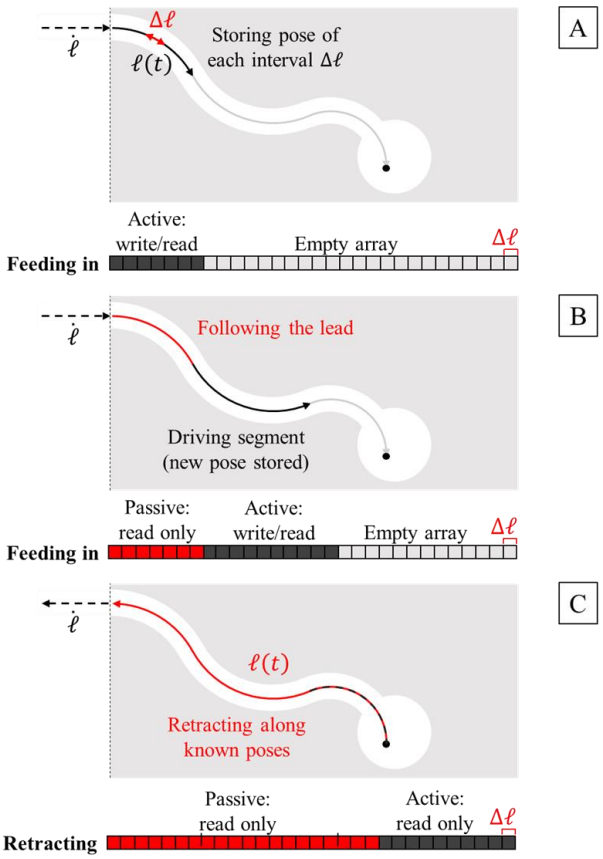

Figure 6. Follow-the-lead algorithm: a. Active segment insertion in the workspace, storing its shape with discrete backbone curvature data; b. Passive segment insertion following the previous shape of the active segment, while the new shape of the advancing active segment is stored; c. During retraction, the stored poses are executed backwards.

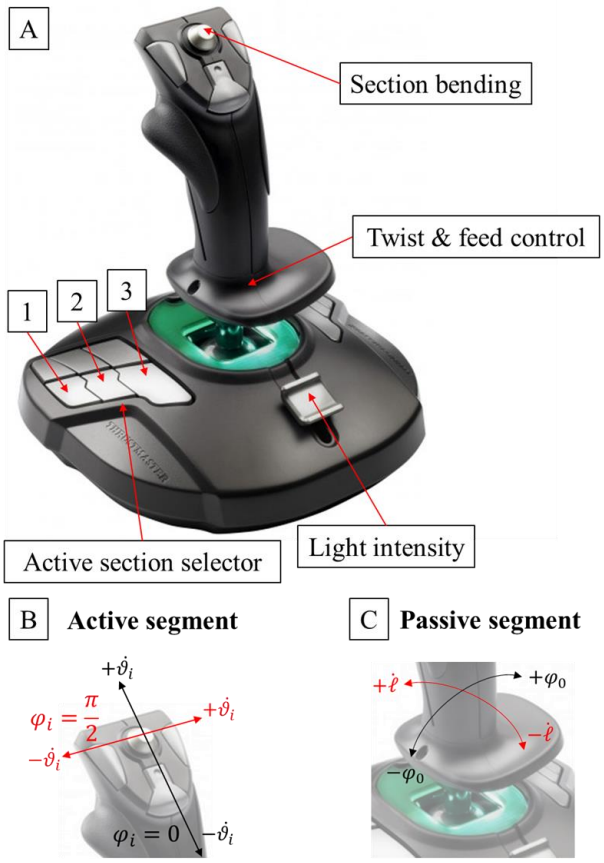

Figure 7. Controller mapping: a. Motion parameters of the continuum robot and corresponding buttons and joysticks on the controller; b. Motion variable mapping for the active segment, with control over the bending speed and direction; c. Motion variable mapping for the passive segment, with control on twist angle and feeding speed.

D. User interfaces

While teleoperation through TCP/IP or keyboard commands is possible, COBRA is equipped with a Thrustmaster T16000 controller for manual operation with a user-friendly mapping of the motion variables (Figure 7) onto this dissimilar-kinematic device [18]. The twist & feed mechanism is controlled through the main stick (wrist of driving hand, Fig. 7c), with forward and backward push controlling feed velocity $\dot{\ell}$ and lateral motion mapped onto the twist φ_0 (up to ±120deg to prevent cable entanglement). A trigger (index finger of driving hand) is configured to enable these controls, ensuring that letting go of the joystick results in a complete stop of all motors. The smaller joystick on top of the main stick (thumb of driving hand, Fig. 7b) is mapped onto the active section, imposing a fixed bending velocity $\dot{\vartheta}_i$ in the φ_i direction the stick is pushed. The thumb joystick controls only the tip when following the leader; alternatively, each active section can be independently selected with the base buttons (fingers of non-driving hand, Fig. 7a), and the remaining controls can be mapped to EE functions (e.g. camera LED intensity, image capture, tool operation).

The immediacy of this interface allows even inexperienced users to quickly learn how to operate the system and reduces the cognitive and physical task load for skilled operators of borescope and continuum robot technologies.

IV. Demonstration

To demonstrate the capabilities of the COBRA system, the robot has been driven by both skilled and unskilled operators in two realistic scenarios: aeroengine inspection and intervention in a pipeline junction. Furthermore, a medical application in throat surgery is reported to show how the proposed design can be adapted to other fields with similar requirements (intervention at reach in enclosed spaces). In this section, we outline the challenges behind these use cases and how COBRA overcomes them.

A. Aerospace

Aircraft engines represent one of the most challenging borescope inspection scenarios. With narrow access ports often in the order of 10mm in diameter, a long reach of several meters required to perform a full inspection, and tortuous paths around the combustion chamber or turbine blades, this scenario requires high mobility, a long reach, and an operator able to drive the system along complex trajectories with the only feedback of the onboard camera. As shown in the pictures in Figure 8, the added mobility of the COBRA active segment simplifies this operation in several stages, from initial insertion (Fig. 8b) to the final inspection (top of Fig. 8d). The LED lights at the tip of the camera probe (Fig. 8c) ensure full functionality even in dark environments. Furthermore, the location of the

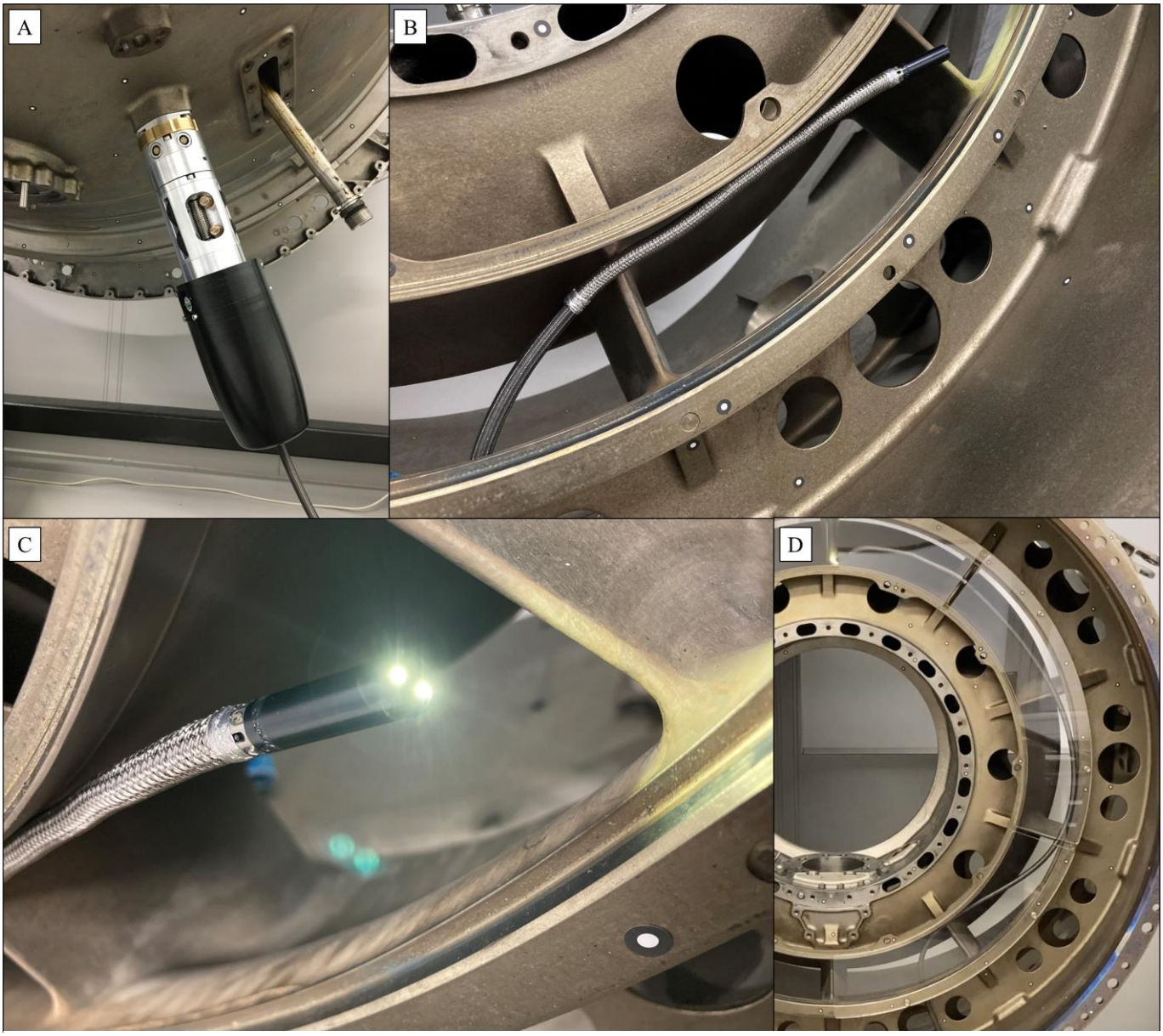

Figure 8. Aerospace demonstration: a. Feed & twist mechanism installed onto the outer case of an aeroengine; b. Active segment entering the engine from a borescope access port; c. EE of the robot performing visual inspection; d. Navigation around the engine core.

access ports often requires operators to stand, crawl, or sit in uncomfortable positions throughout an entire inspection to manually feed the borescope in, leading to health and safety issues that can range from mild discomfort to repetitive strain injuries and chronic pain. This problem can be fully circumvented by installing the feed & twist mechanism directly onto the access port (Fig. 8a).

B. Nuclear

The second demonstration of COBRA, shown in Figure 9, relates to pipeline inspection in nuclear power generation installations. After attaching the twist & feed mechanism onto an opening (Fig. 9a), the continuum robot was driven through the pipes (Fig. 9b), inspecting difficult to reach regions (e.g., due to corners, Fig. 9c) and pipe ceiling (Fig. 9d). The latter highlights the advantages of the active segment: a full tip bend around a corner while suspended, as in Figure 9c, cannot be achieved by a conventional borescope, limiting the number of reachable pipe lines; furthermore, a conventional borescope would not be able to lift its EE as in Figure 9d, thus either not achieving full inspection or only giving a distant visual feedback with limited information (i.e. low quality image, out of range for depth measurement or intervention). At the same time, a fully actuated continuum robot might be hindered by the need to achieve follow-the-lead motion over a long reach within this target environment, thus leading to hybrid designs like COBRA as the only solution for such operations.

C. Throat surgery

In this application, illustrated in Figure 10, we show how the modularity of COBRA enables medical applications with a novel EE, designed for minimally invasive throat surgery. Existing robotic surgical systems, such as the da Vinci [19], are usually constrained to a specific application or do not have

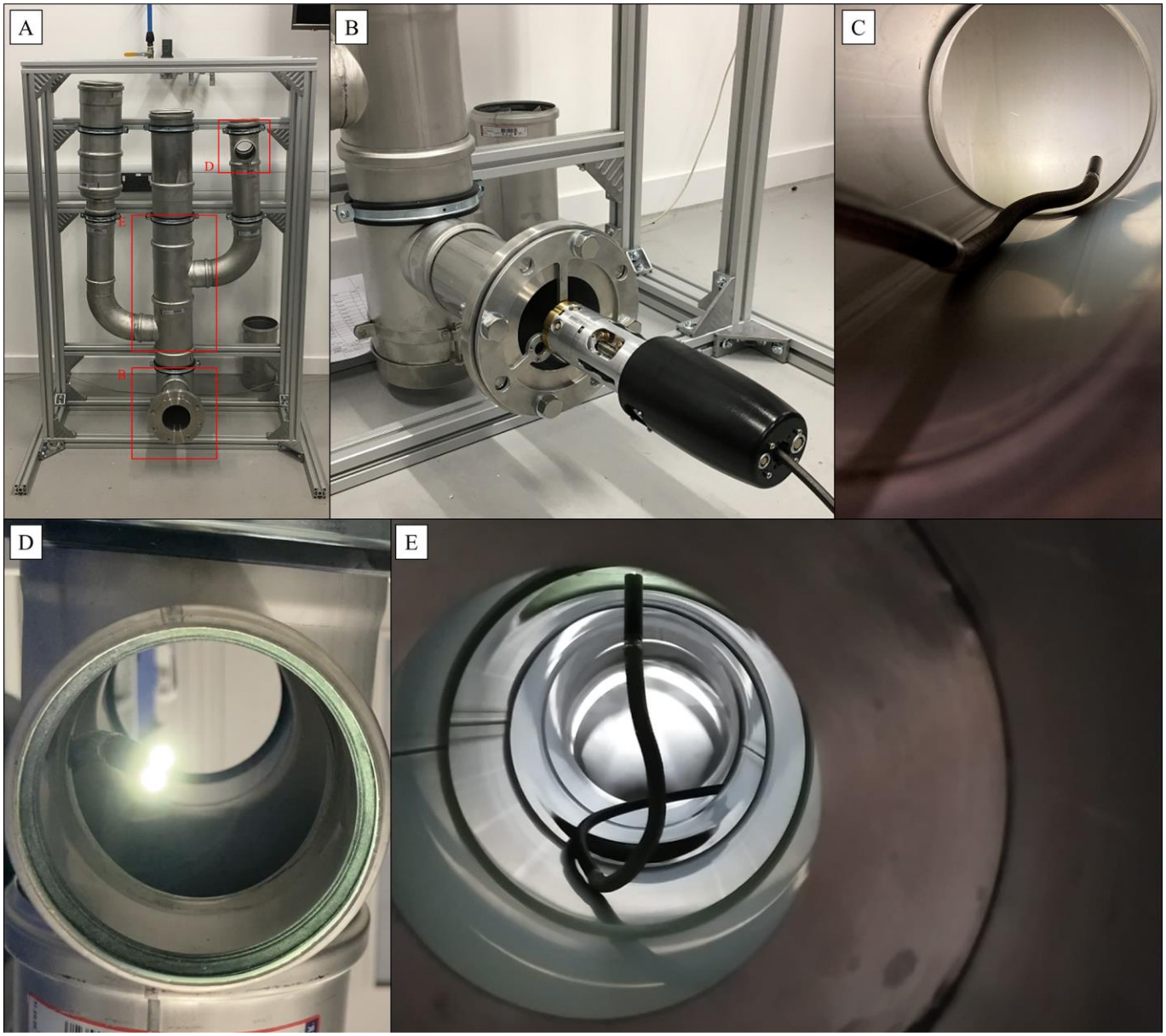

Figure 9. Nuclear demonstration: a. Inspection target (vertical layout); b. Feed & twist mechanism installation; c. Pipeline navigation; d. Camera EE with LED lights on; e. Lifting the EE with the active segment to perform ceiling inspection (horizontal layout).

enough flexibility or degrees of freedom for this specific application. Endoscopes are instead limited to two DoFs and one single task at a time. As such, our design has been tailored to provide not only EE multitasking and multiple DoFs, but also enabling precise positioning and control over a small region inside the throat to assist in throat cancer surgeries.

The EE holds an inspection camera and forks into two miniature active sections (MAS), which are scaled-down (6mm) 5-vertebra active segments that provide independent 2-DoF mobility for two tools: a surgical diathermy cutter and a tweezer (Fig. 10). This design enables the use of the main COBRA body for coarse EE positioning, whereas the MAS can be finely tuned to a specific region of interest within the throat with their own tendon mechanisms, guided through the onboard camera feedback.

The diathermy cutter is activated by an insulated cable that passes through the center of the MAS and is connected to an external diathermy unit for surgery. The tweezers work via a symmetric tendon-driven 4-linkage mechanism, spring-loaded to its open configuration (see Fig. 10a). The linkage is optimized for the tweezer tendon to compress the spring with a minimum load and achieve the grasping force required to remove the tissue cut with the diathermy cutter without compromising the configuration of the EE nor the active section of COBRA. The advantage of having 2 DOF on each MAS is that the diathermy cutter and the tweezers can perform actions simultaneously in the center or separately by moving the MAS away from each other (see Fig. 10a-b). Both MAS and the camera have an initial tilt angle for optimal camera field of view and for maximizing the workspace intersection of the two MAS. With this design, the robot is able to perform the surgical procedures that are daily encountered when dealing with throat cancer subjects, such as cauterizing or cutting tissue (e.g. tumors, injured tissue) and removing it from the body.

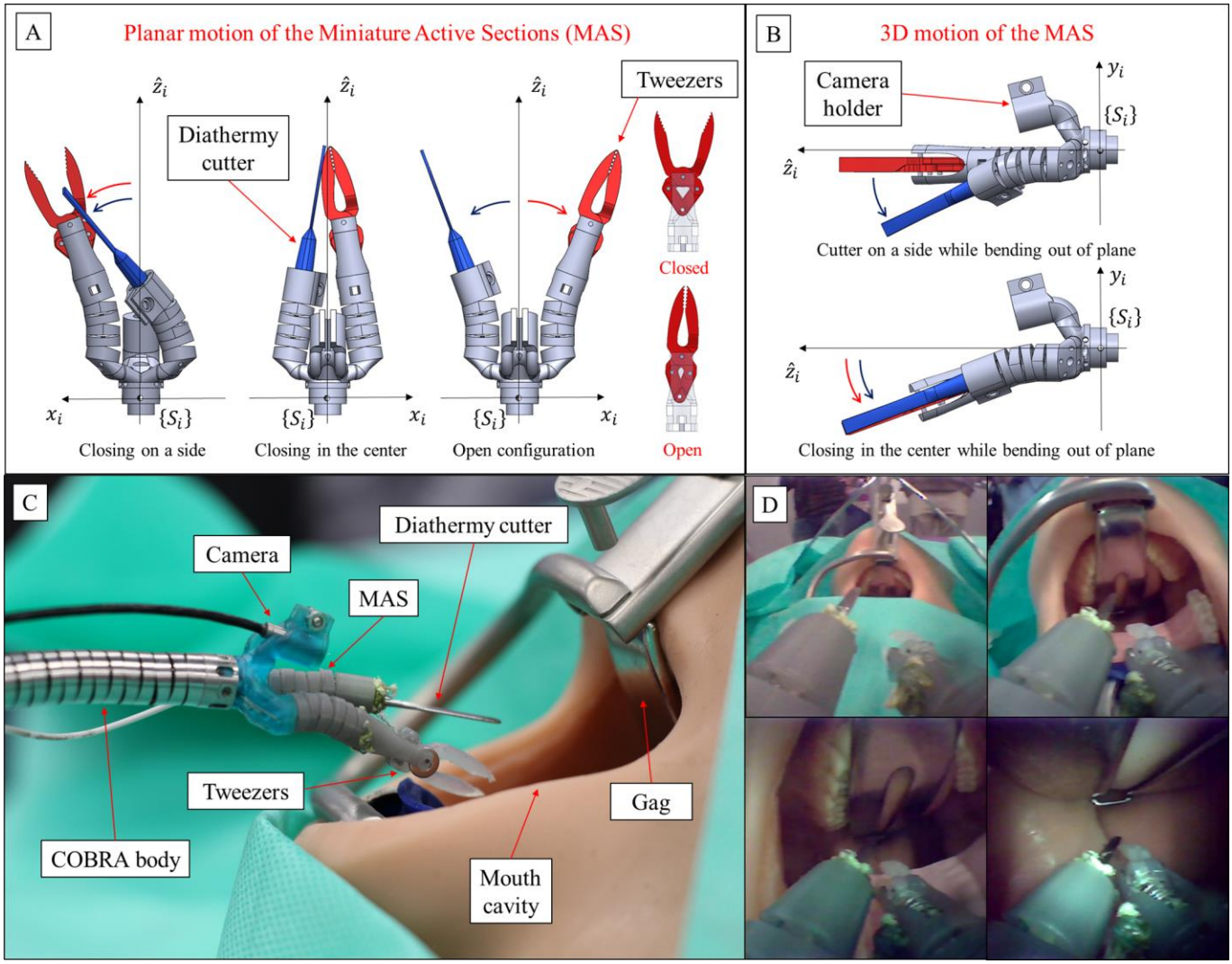

Figure 10. Medical demonstration: a. Top view of the end-effector design; b. Side view of the end-effector design; c. Close-up of the end-effector accessing the throat via the mouth cavity; d. Snapshots of the end-effector camera view during operation, with the continuum robot accessing the throat and positioning in a specific region of interest.

Using a soft polymeric head and neck replica, this robot was proven to successfully access the throat through the proper manipulation of the main COBRA body (Fig. 10d), and MAS operation was validated on organic tissue. Consequently, this application shows the versatility of COBRA, making it a suitable design for difficult-to-access environments where either single or multiple tasks are performed in-situ.

V. Conclusion

In this work, we introduced COBRA, a novel continuum robot design for intervention in hard-to-reach areas. By combining design solutions from both borescope and continuum robot technologies, the proposed design overcomes many of the intrinsic limitations of those systems:

- A 6-DoF active segment, whose shape is fully controlled, enables navigation through complex environments.
- A passive segment with high compliance is used to achieve a long reach, overcoming backbone length constraints of fully actuated designs. As such, the proposed design achieves a length to diameter ratio that is significantly higher than conventional continuum robots (i.e., 625, up to 125-150 in active slender robots)
- A modular actuation with a motor pack for the tendon-driven segment and a separate mechanism to drive the passive parts ensures enough DoF to deliver the EE to the target workspace, while enabling an intuitive mapping to a joystick controller for a user-friendly interface that significantly reduces task complexity for operators.

These advantages have been demonstrated in two real-case scenarios for nuclear and aerospace, in which a prototype of the proposed robot (5m in length, less than 9mm in diameter, 6 DoF at the active segment, 2 DoF at the passive segment) outperformed both borescopes and continuum robots. The modularity of the novel design also allows for different configurations (e.g., multiple passive or active segments) to adapt COBRA for a large variety of other applications such as surgical robotics, as highlighted in the reported medical application.

In the reported example a human operator guides the robot throughout the operation, compensating for the limited onboard sensing (EE camera) and errors due to the unknown shape of the

passive section (e.g. variation of tendon length and thus active section shape due to passive section bending). However, future development will focus on enabling automated operation with SLAM techniques or shape sensing (e.g. with fiber Bragg grating).

ACKNOWLEDGMENTS

We would like to thank Dr Oladejo Olaleye for assisting us in the development and demonstration of the medical COBRA prototype, providing us with his knowledge, experience, and feedback on ENT, head & neck, and transoral surgery as a Robotic Surgeon at the University Hospitals of Leicester NHS Trust.

APPENDIX

Supplementary videos can be found online at:

- https://www.youtube.com/watch?v=BlhULsPVgLU
- https://www.youtube.com/watch?v=GJoAQ1KxaVw&t=1s

REFERENCES

[1] C.Y. Wong, P. Seshadri, and G.T. Parks. "Automatic borescope damage assessments for gas turbine blades via deep learning." In *AIAA Scitech 2021 Forum*, pp. 1488, 2021. https://doi.org/10.2514/6.2021-1488

[2] J. Aust et al., "Automated defect detection and decision-support in gas turbine blade inspection." *Aerospace* vol. 8, no. 2, pp. 30, 2021.

[3] C. Markman, R.J. Zawoysky, *Generator in-situ inspections*. GER-3954C, GE Energy, 2012.

[4] J. Aust, D. Pons, and A. Mitrovic, "Evaluation of Influence Factors on the Visual Inspection Performance of Aircraft Engine Blades." *Aerospace* vol. 9, no. 1, pp. 18, 2022.

[5] I.D. Walker, H. Choset, and G.S. Chirikjian. "Snake-like and continuum robots." *Springer handbook of robotics*, pp. 481-498. Springer, Cham, 2016.

[6] P. Rao, Q. Peyron, S. Lilge, and J. Burgner-Kahrs. "How to model tendon-driven continuum robots and benchmark modelling performance." *Frontiers in Robotics and AI* vol. 7, pp. 223, 2021.

[7] R.J. Webster III, and B.A. Jones. "Design and kinematic modeling of constant curvature continuum robots: A review." *International Journal of Robotics Research* vol. 29, no. 13, pp. 1661-1683, 2010.

[8] M. Russo et al., "Task-oriented optimal dimensional synthesis of robotic manipulators with limited mobility." *Robot. Comp. Int. Manuf.* vol. 69, p. 1020962021. https://doi.org/10.1016/j.rcim.2020.102096

[9] X. Dong et al., "Continuum robots collaborate for safe manipulation of high-temperature flame to enable repairs in extreme environments." *IEEE/ASME Transactions on Mechatronics*, 2021. https://doi.org/10.1109/TMECH.2021.3138222

[10] A. Mohammad, M. Russo, Y. Fang, X. Dong, D. Axinte, J. Kell, "An efficient follow-the-leader strategy for continuum robot navigation and coiling." *IEEE Robotics and Automation Letters* vol. 6, no. 4, pp. 7493-7500, 2021. https://doi.org/10.1109/LRA.2021.3097265

[11] M. Russo et al., "Cooperative continuum robots: Enhancing individual continuum arms by reconfiguring into a parallel manipulator", *IEEE Robotics and Automation Letters* vol. 7, no. 2, pp. 1558-1565, 2021. https://doi.org/10.1109/LRA.2021.3139371

[12] E. Amanov, T.D. Nguyen, and J. Burgner-Kahrs, "Tendon-driven continuum robots with extensible sections—A model-based evaluation of path-following motions." *International Journal of Robotics Research* vol. 40, no. 1, pp. 7-23, 2019. https://doi.org/10.1177/0278364919886047

[13] J. Burgner-Kahrs, D.C. Rucker, and H. Choset, "Continuum robots for medical applications: A survey." *IEEE Transactions on Robotics* vol. 31, no. 6 pp.1261-1280, 2015. https://doi.org/10.1109/TRO.2015.2489500

[14] X. Dong, M. Raffles, S. Cobos-Guzman, D. Axinte, and J. Kell. "A novel continuum robot using twin-pivot compliant joints: design, modeling, and validation." *Journal of Mechanisms and Robotics* vol. 8, no. 2, 2016.

[15] K. Oliver-Butler, J. Till, and C. Rucker. "Continuum robot stiffness under external loads and prescribed tendon displacements." *IEEE Transactions on Robotics* vol. 35, no. 2, pp. 403-419, 2019.

[16] D.B. Camarillo et al., "Mechanics modeling of tendon-driven continuum manipulators." *IEEE Transactions on Robotics* vo. 24, no. 6, pp. 1262-1273, 2008. https://doi.org/10.1109/TRO.2008.2002311

[17] H. Choset and W. Henning, "A follow-the-leader approach to serpentine robot motion planning," *Int. J. Aerosp. Eng.*, vol. 12, no. 2, pp. 65-73, 1999.

[18] K. Kim, W. K. Chung, and I. H. Suh, "Accurate force reflection for kinematically dissimilar bilateral teleoperation systems using instantaneous restriction space," in *Proc. IEEE Int. Conf. Robot. Autom.*, Orlando, Florida, 2006, pp. 3257-3262.

[19] C. Freschi, V. Ferrari, F. Melfi, M. Ferrari, F. Mosca, and A. Cuschieri. "Technical review of the da Vinci surgical telemanipulator." *The International Journal of Medical Robotics and Computer Assisted Surgery* 9, no. 4, pp. 396-406, 2013.